Berkala **PENELITIAN HAYATI**

ISSN: 08526834 | E-ISSN:2337-389X
Volume 29| No. 2| August|2023

Original Article

Virtual prediction of Brown Rice Gamma Oryzanol as anti-inflammation via COX-1 and COX-2 inhibitions

Christine Natalia Palis[1,2], Anna Safitri[1,2], Ernanin Dyah Wijayanti[2,3,4], Fatchiyah Fatchiyah[2,3*]
[1]Chemistry Department, Faculty of Mathematics and Natural Sciences, Brawijaya University, Malang, 65145, Indonesia
[2]Research Centre for Smart Molecules of Natural Genetic Resources, Brawijaya University, Malang, 65145, Indonesia
[3]Biology Department, Faculty of Mathematics and Natural Sciences, Brawijaya University, Malang, 65145, Indonesia
[4]Health Polytechnique of Putra Indonesia Malang, Malang, 65123, Indonesia

Abstract

Brown rice gamma oryzanol (GO) is an important bioactive compound with numerous potential health functions, such as anti-inflammatory and anti-diabetic. Cyclooxygenase (COX) is the enzyme that mediates the biological transformation of arachidonic acid (ARA) into prostaglandins (PGs) in the mechanism of inflammation. This study purposed to identify the potency of gamma oryzanol of brown rice as an anti-inflammatory compound via COX-1 and COX-2 inhibition. The three-dimensional structure of COX-1 and COX-2 was determined by binding affinity calculations from virtual molecular docking with gamma oryzanol ligand through in silico study. Arachidonic acid as native ligand of COX-1/COX-2 was performed as a control in this study. Gamma oryzanol (CIS 5282164) and arachidonic acid (CIS 444899) were downloaded in 3D-SDF format from the PubChem database. The three-dimensional model of COX-1 and COX-2 was acquired from the protein data bank (www.rscb.org) in PDB format. The molecular docking was performed by Vina Wizard integrated on PyRx version 0.8. The interaction between GO and COX-1/COX-2 was visualized using the Discovery Studio version 2022 software. Molecular dynamics (MD) simulation also used to analyze the stability of the protein-ligand complex. The results showed that brown rice gamma oryzanol binds to COX-1 and COX-2 at many active sites with strongest binding affinity compared to arachidonic acid, with energy binding -7.8 kcal/mol and -6.2 kcal/mol, respectively. This in silico study concluded that brown rice gamma oryzanol has potential function as an anti-inflammatory activity through COX-1 and COX-2 catalysis reduction.

Keywords: Anti-inflammatory, brown-rice, cyclooxygenase, gamma oryzanol
Received: March 4, 2023 Revised: May 19, 2023 Accepted: May 24, 2023

Introduction

Gamma oryzanol (GO) is a bioactive compound found in grain and brown rice (*Oryza sativa* L.) bran (Francisqueti et al., 2017). The GO content in rice bran is 13-20 times (w/w) higher compared to tocopherols and tocotrienols (Srikaeo, 2014). According to Hongsibsong et al. (Hongsibson et al., 2016), raw brown rice samples contain 34.98-71.13 µg/g of total GO. In recent studies, GO has the potential as a pharmaceutical, such as an antioxidant, anti-inflammatory, anti-diabetic and anti-cancer. Gamma oryzanol is an antioxidant polyphenol that plays a significant role as an anti-inflammatory compound (Mastinu et al., 2019; Rao et al., 2016). Previous studies have shown that GO compounds can prevent inflammation by decreasing the secretion of pro-inflammatory mediators by macrophages (Rao et al., 2016). Also, GO has been reported as a suppressor of cyclooxygenase (COX-2) expression (Shin et al., 2017).

The COX is an enzyme that mediates inflammation responses by prostaglandins (Dewi, 2016). The COX-2 enzyme is a significant isoenzyme in the inflammatory process but the data showed that prostanoids produced by COX-1 also play a role in inflammation (Smith & Langenbach, 2001). Arachidonic acid (ARA) is a substrate of COX enzymes that modulates the synthesis of prostaglandin (Krisnamurti et al., 2020). The interaction between ARA on the COX active sites, produced prostaglandin G2 (PGG2). The PGG2 has an important role as the first intermediate on biological transformation of the prostaglandins and thromboxane, that are involved with the inflammation (Goltsov et al., 2020).

The COX consist of three domains, which are the epidermal growth factor, the membrane binding, and the catalytic domains, where the both sides of the heme COX prosthetic group contain the COX and active site (Rouzer & Marnett, 2009). The membrane binding domain of this enzyme consists of an L-shaped channel structure formed by hydrophobic area. At the top of the L-shaped channel, the COX active site is located in the hydrophobic area. Substrates and inhibitors enter the channel to up-regulate the activated COX active site (Rouzer & Marnett, 2003).

The sequences of COX-1 and COX-2 are closely analogous and their three-dimensional structures are comparable (Tomić et al., 2017). The typical anti-inflammatory drugs inhibit and block the selectivity of COX-1 and/or COX-2 (Gunaydin & Bilge, 2018). This study focused on assessing the anti-inflammatory potential of GO against COX-1 and/or COX-2 using virtual molecular docking through an in-silico study.

*Corresponding Author:
Fatchiyah Fatchiyah
Department of Biology, Faculty of Mathematics and Natural Sciences, Brawijaya University. Research Center of Smart Molecule of Natural Genetics Resources, Brawijaya University
Phone: 0341-575841 Fax: 0341-575841
E-mail: fatchiya@ub.ac.id

Method

Protein and ligands preparation

The three-dimensional model of the enzyme was acquired from the protein data bank (www.rscb.org) in PDB format with PDB ID: 1PTH for COX-1 and PDB

http://dx.doi.org/10.23869/bphjbr.29.2.20233
Published by © PBI East Java. Open Access www.berkalahayati.org

ID: 6COX for COX-2. The water molecules and native ligands of the protein were removed using Biovia Discovery Studio Visualizer 2022. The three-dimension structure of GO compound (CID 5282164) and ARA (CID 444899) were obtained from PubChem in SDF format, then converted to PDB format using open babel. The ligands were prepared using Open Babel integrated into PyRx version 0.8 by minimizing the energy (Wijayanti et al., 2021).

Molecular docking and visualization

The molecular docking was performed by Autodock Vina integrated into PyRx ver.0.8. The center grid box coordinates were x: 35.9880, y: 45.8102, z: 71.6363, and the dimensions were x: 82.6939 Å, y: 43.8164 Å, and z: 31.4436 Å. The docking results were saved in PDB format, and the binding affinity data of the protein-ligands were saved in CSV format. The protein-ligand interaction was visualized and analyzed using Biovia Discovery Studio Visualizer 2022. Results were analyzed to determine the energy level and the types of binding area.

Molecular dynamic simulation

The ligand topology is determined based on ligand information (HETATM) and generated using PRODRG2 server (http://davapc1.bioch.dundee.ac.uk/cgi-bin/prodrg). Molecular dynamics was performed using the Gromacs provider via Webgro: Molecular Simulation web server (https://simlab.uams.edu/). The simulation parameters include forcefield: water model: SPC, box type: Cubic, salt type: NaCl + Neutralize + add 0.15 M salt, temperature 310K, and simulation time: 20 ns. The molecular dynamic simulation results were plotted using Graphpad Prism 9.0 version.

The drug likeness, biological activity, ADME, and toxicity prediction

The drug-likeness, and biological activity prediction of GO were predicted using molinspiration (https://www.molinspiration.com/) and PASS online (http://way2drug.com/passonline). Adsorption, Distribution, Metabolism and Excretion (ADME) of GO were analyzed by the SwissADME website (http://www.swissadme.ch/). The toxicity prediction of GO was performed by ProTox (https://tox-new.charite.de/protox_II/index.php?site=home).

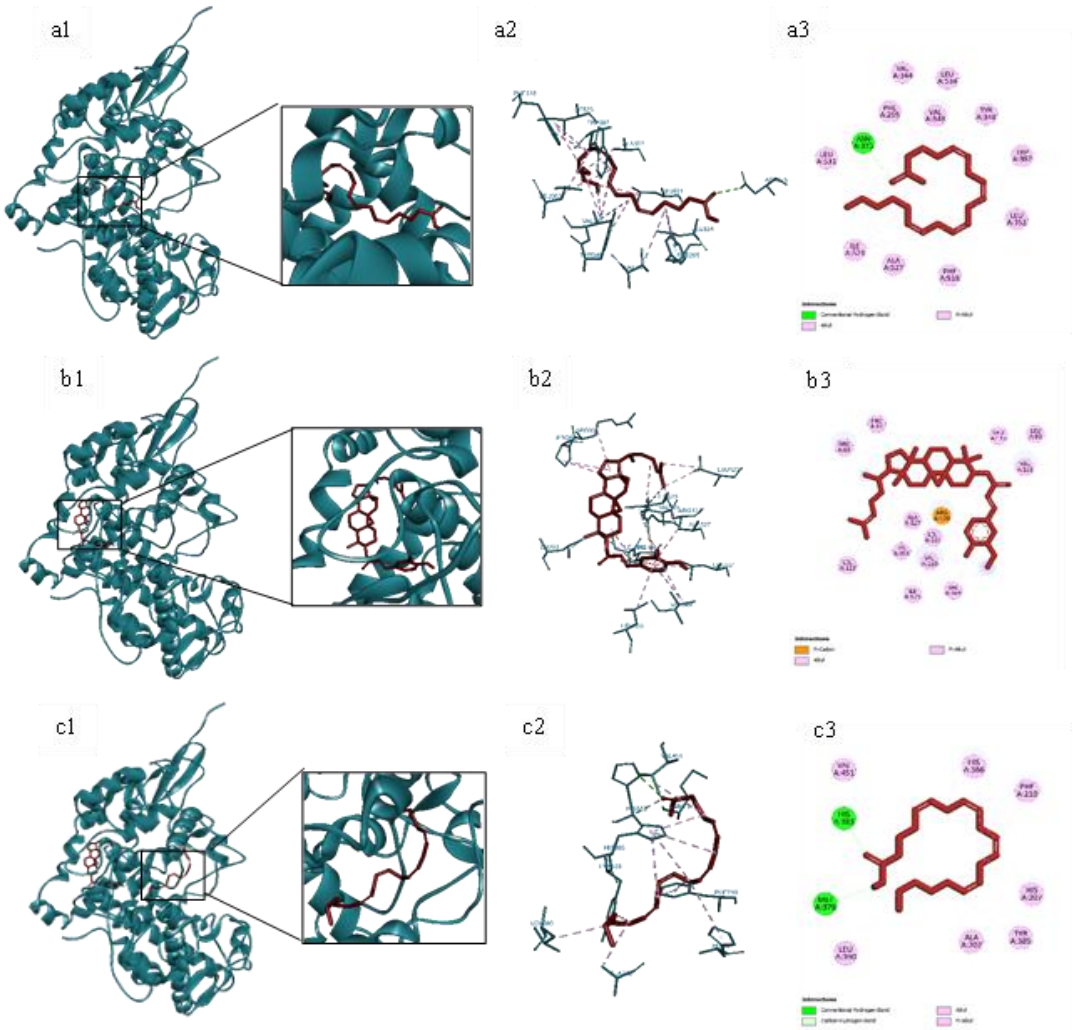

Figure 1. The molecular interaction prediction among the ligands and COX-1 protein. The ligand-protein complex was represented in alphabetic legend, arachidonic acid (a), gamma oryzanol (b), gamma oryzanol-COX-1 + arachidonic acid (c). Blue color represents COX-1 protein, and the red color is the ligands.

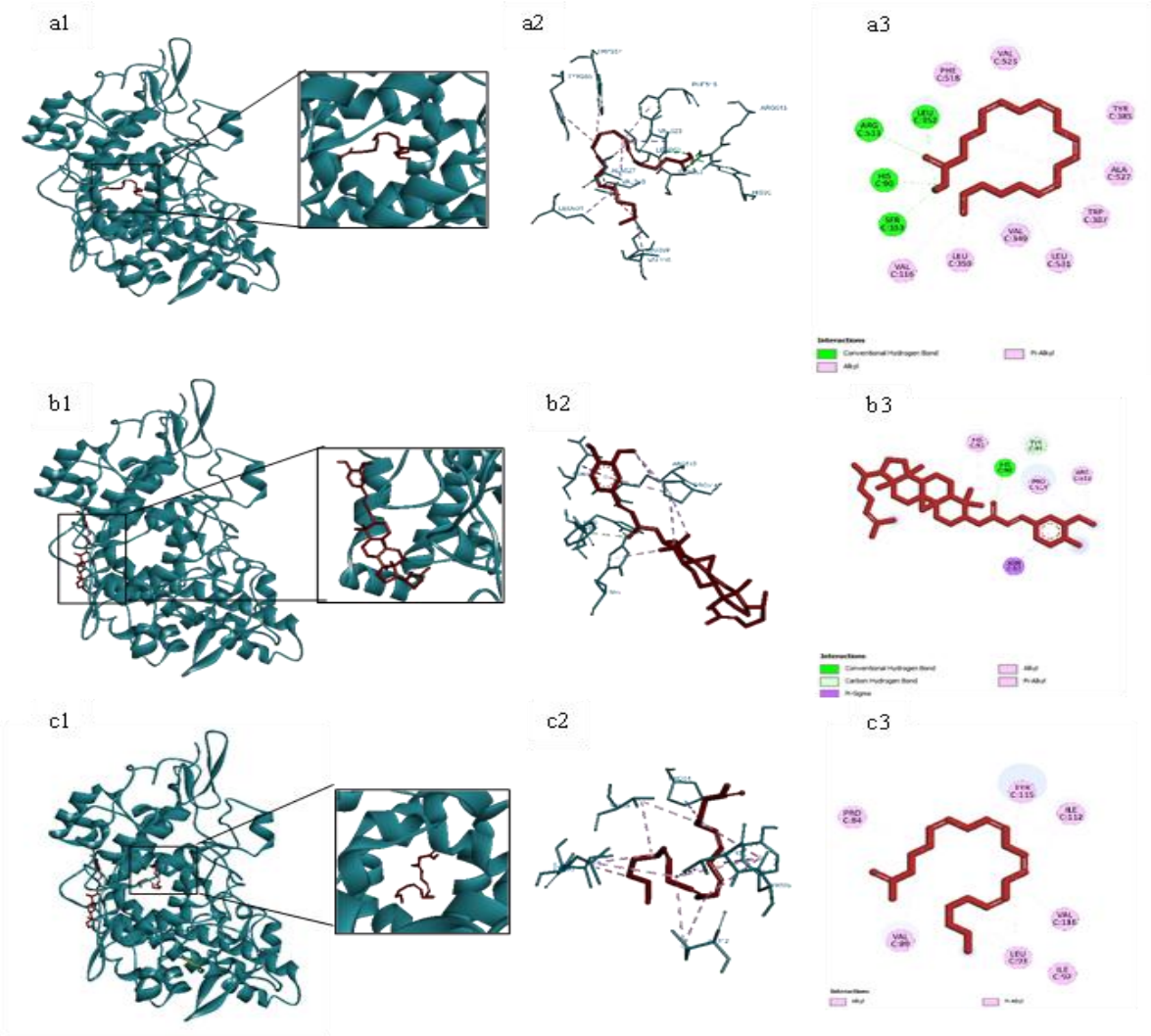

Figure 2. In silico molecular docking interaction between arachidonic acid (a), gamma oryzanol (b) with COX-2 and (c) gamma oryzanol-COX-2 + arachidonic acid complexes. The 3D and 2D structure of ligand-protein complexes were demonstrated with numerical legend. Blue color is COX-2 protein and the red color is the ligands.

Results

Molecular docking

The ligands-protein interaction was shown in Figure 1 and 2. According to the interaction of GO, ARA and COX-1 enzyme (Table 1), there were three different types of chemical bonds that can be found in ligand-protein interaction, such as hydrogen, hydrophobic, and electrostatic bonds. One conventional hydrogen bond, involving the ASN375 amino acid residue, and hydrophobic bonds were formed between ARA and COX-1 (Fig. 1a). The amino acid residues involved in hydrophobic bond formation between ARA-COX 1 complex interaction were PHE205, VAL344, VAL349, TYR348, VAL349, LEU352, TRP387, PHE518, ILE523, ALA527, and LEU531.

In the GO-COX-1 interaction, there were one electrostatic bond involving ARG120 residue and some hydrophobic bonds involving 13 amino acid residues including PRO84, LEU115, VAL116, LEU93, VAL349, ILE523, VAL119, ARG120, LEU123, ARG83, LEU359, ALA527, and LEU531. Among these residues, VAL349, ILE523, ALA527, and LEU531 were same as residues involved in ARA-COX-1 interaction.

The interaction of GO with COX-1 prevents ARA from binding to the same COX-1 residue as before. In the presence of GO, ARA-COX-1 interactions were formed by hydrogen bonds involving MET379 and HIS383, as well as hydrophobic bonds involving LEU390, VAL451, ALA202, HIS207, PHE210, and HIS386. The binding affinity produced from ARA-COX-1, GO-COX-1, and GO-COX-1 + ARA were -7.6 kcal/mol, -7.8 kcal/mol, and -7.0 kcal/mol, respectively. The GO-COX-1 + ARA interaction showed the lowest binding affinity among other interactions

.

Table 1. Interaction of ligands and COX-1 complexes

Complexes (binding affinity (kcal/mol))	Interaction	Category	Types	Distance (Å)
Arachidonic acid (Native Ligand)-COX-1 (-7.6)	A:ASN375:ND2 - N:UNK1:O	Hydrogen	Conventional Hydrogen Bond	3.32
	N:UNK1 - A:VAL349	Hydrophobic	Alkyl	4.49
	N:UNK1 - A:LEU352	Hydrophobic	Alkyl	4.97
	N:UNK1 - A:ILE523	Hydrophobic	Alkyl	4.92
	N:UNK1 - A:VAL349	Hydrophobic	Alkyl	4.86
	N:UNK1:C - A:VAL349	Hydrophobic	Alkyl	4.70
	N:UNK1:C - A:ALA527	Hydrophobic	Alkyl	3.89
	N:UNK1:C - A:LEU531	Hydrophobic	Alkyl	4.74
	N:UNK1 - A:VAL344	Hydrophobic	Alkyl	5.25
	N:UNK1 - A:LEU534	Hydrophobic	Alkyl	4.50
	A:ALA527 - N:UNK1	Hydrophobic	Alkyl	4.27
	A:PHE205 - N:UNK1	Hydrophobic	Pi-Alkyl	4.78
	A:TYR348 - N:UNK1	Hydrophobic	Pi-Alkyl	4.66
	A:TRP387 - N:UNK1	Hydrophobic	Pi-Alkyl	5.28
	A:PHE518 - N:UNK1	Hydrophobic	Pi-Alkyl	4.73
Gamma-oryzanol-COX-1 (-7.8)	A:ARG120:NH1 - N:UNK1	Electrostatic	Pi-Cation	3.47
	N:UNK1:C - A:PRO84	Hydrophobic	Alkyl	4.23
	N:UNK1:C - A:LEU115	Hydrophobic	Alkyl	4.40
	N:UNK1:C - A:VAL116	Hydrophobic	Alkyl	4.02
	N:UNK1:C - A:LEU93	Hydrophobic	Alkyl	4.77
	N:UNK1:C - A:VAL349	Hydrophobic	Alkyl	4.90
	N:UNK1:C - A:ILE523	Hydrophobic	Alkyl	5.22
	N:UNK1 - A:VAL119	Hydrophobic	Alkyl	5.44
	N:UNK1:C - A:VAL119	Hydrophobic	Alkyl	4.86
	N:UNK1:C - A:ARG120	Hydrophobic	Alkyl	4.40
	N:UNK1:C - A:LEU123	Hydrophobic	Alkyl	4.61
	A:ARG83 - N:UNK1	Hydrophobic	Alkyl	5.00
	A:PRO84 - N:UNK1	Hydrophobic	Alkyl	5.04
	A:VAL116 - N:UNK1	Hydrophobic	Alkyl	4.20
	N:UNK1 - A:VAL116	Hydrophobic	Pi-Alkyl	5.47
	N:UNK1 - A:VAL349	Hydrophobic	Pi-Alkyl	5.15
	N:UNK1 - A:LEU359	Hydrophobic	Pi-Alkyl	5.21
	N:UNK1 - A:ALA527	Hydrophobic	Pi-Alkyl	4.38
	N:UNK1 - A:LEU531	Hydrophobic	Pi-Alkyl	4.99
Gamma oryzanol-COX-1 + Arachidonic acid (-7.0)	N:UNK1:H - A:MET379:O	Hydrogen	Conventional Hydrogen Bond	2.71
	A:HIS383:ND1 - N:UNK1:O	Hydrogen	Conventional Hydrogen Bond	2.96
	A:HIS383:CA - N:UNK1:O	Hydrogen	Carbon Hydrogen Bond	3.27
	N:UNK1:C - A:LEU390	Hydrophobic	Alkyl	4.29
	N:UNK1 - A:VAL451	Hydrophobic	Alkyl	5.25
	A:ALA202 - N:UNK1	Hydrophobic	Alkyl	4.18
	A:HIS207 - N:UNK1	Hydrophobic	Pi-Alkyl	5.46
	A:PHE210 - N:UNK1	Hydrophobic	Pi-Alkyl	5.22
	A:HIS386 - N:UNK1	Hydrophobic	Pi-Alkyl	4.46

The docking experiments revealed the interaction of ARA and GO with the COX-2 receptor. Table 2 represents the binding affinity scores of the docked complexes. The native ligand, ARA, showed interaction residues with COX-2 with a binding affinity score of -8.0 kcal/mol binds, through hydrogen bonds, namely HIS90, LEU352, SER353 and ARG513, and hydrophobic bonds with VAL16, VAL349, LEU359, TRP387, TYR385, PHE518, ALA527, LEU531 amino acid residues. The GO of brown rice showed significant interaction with COX-2 with a binding affinity score of -6.2 kcal/mol.

The GO-COX-2 interactions were formed by hydrogen and hydrophobic bond. The residues involved in hydrogen bonds were HIS90 and TYR91, while the hydrophobic bonds involving ASN87, PRO514, ARG513, and HIS95 residues. The binding affinity produced was -6.2 kcal/mol.

The GO-COX-2 and ARA complex showed no hydrogen bond interaction with any of the amino acid residues. Arachidonic acid binds to the GO-COX-2 complex through hydrophobic bond interactions with -5.2 kcal/mol binding affinity. The interacting residues of this complex are PRO84, VAL89, ILE92, LEU93, ILE112, TYR115, and VAL116.

Table 2. The interaction of ligands and COX-2 complex

Complexes (binding affinity (kcal/mol))	Interaction	Category	Types	Distance (Å)
Arachidonic acid-COX-2 (-8.0)	N:UNK1:H - C:LEU352:O	Hydrogen	Conventional	2.98
	N:UNK1:H - C:SER353:O	Hydrogen	Conventional	2.61
	C:HIS90:HE2 - N:UNK1:O	Hydrogen	Conventional	1.96
	C:ARG513:HH11 - N:UNK1:O	Hydrogen	Conventional	3.09
	C:ARG513:HH12 - N:UNK1:O	Hydrogen	Conventional	2.94
	N:UNK1 - C:LEU352	Hydrophobic	Alkyl	5.24
	N:UNK1 - C:VAL523	Hydrophobic	Alkyl	4.36
	N:UNK1 - C:VAL349	Hydrophobic	Alkyl	3.89
	N:UNK1 - C:LEU352	Hydrophobic	Alkyl	5.29
	N:UNK1 - C:VAL349	Hydrophobic	Alkyl	4.14
	N:UNK1 - C:LEU531	Hydrophobic	Alkyl	4.15
	N:UNK1:C - C:VAL116	Hydrophobic	Alkyl	4.46
	N:UNK1:C - C:VAL349	Hydrophobic	Alkyl	5.12
	N:UNK1:C - C:LEU359	Hydrophobic	Alkyl	4.27
	C:ALA527 - N:UNK1	Hydrophobic	Alkyl	5.19
	C:ALA527 - N:UNK1	Hydrophobic	Alkyl	3.95
	C:TYR385 - N:UNK1	Hydrophobic	Pi-Alkyl	4,90
	C:TRP387 - N:UNK1	Hydrophobic	Pi-Alkyl	5.39
	C:PHE518 - N:UNK1	Hydrophobic	Pi-Alkyl	4.95
Gamma Oryzanol-COX 2 (-6.2)	C:HIS90:HD1 - N:UNK1:O	Hydrogen	Conventional	2.21
	C:TYR91:CA - N:UNK1:O	Hydrogen	Carbon Hydrogen	3.54
	C:ASN87:CB - N:UNK1	Hydrophobic	Pi-Sigma	3.74
	N:UNK1:C - C:PRO514	Hydrophobic	Alkyl	4.26
	N:UNK1:C - C:ARG513	Hydrophobic	Alkyl	4.05
	N:UNK1:C - C:PRO514	Hydrophobic	Alkyl	5.05
	C:PRO514 - N:UNK1	Hydrophobic	Alkyl	4.95
	N:UNK1 - C:PRO514	Hydrophobic	Pi-Alkyl	5.13
	C:HIS95 - N:UNK1:C	Hydrophobic	Pi-Alkyl	3.50
Gamma Oryzanol-COX-2 + Arachidonic Acid (-5.8)	N:UNK1 - C:ILE112	Hydrophobic	Alkyl	4.56
	N:UNK1 - C:LEU93	Hydrophobic	Alkyl	5.08
	N:UNK1 - C:ILE112	Hydrophobic	Alkyl	4.95
	N:UNK1 - C:VAL116	Hydrophobic	Alkyl	4.80
	N:UNK1 - C:VAL89	Hydrophobic	Alkyl	4.28
	N:UNK1 - C:LEU93	Hydrophobic	Alkyl	4.27
	N:UNK1:C - C:ILE92	Hydrophobic	Alkyl	4.33
	N:UNK1 - C:PRO84	Hydrophobic	Alkyl	4.82
	N:UNK1 - C:VAL89	Hydrophobic	Alkyl	4.44
	C:TYR115 - N:UNK1	Hydrophobic	Pi-Alkyl	3.97
	C:TYR115 - N:UNK1	Hydrophobic	Pi-Alkyl	4.48
	C:TYR115 - N:UNK1	Hydrophobic	Pi-Alkyl	5.45
	C:TYR115 - N:UNK1	Hydrophobic	Pi-Alkyl	4.96

Molecular dynamic simulation

Molecular dynamic simulation was carried out to identify the stability of the molecular interaction in each complex (Nafisah et al., 2022). The molecular dynamic simulation parameters are radius of gyration (Rg), root-mean-square deviation (RMSD), root-mean-square fluctuation (RMSF), and number of hydrogen bonds (Vishvakarma et al., 2022). Figure 4a shows the RMSD value of GO-COX-1 and GO-COX-1 + ARA complex. Figure 4a confirms that every complex attained a stable state throughout the simulation after 10 ns.

The RMSF plots are shown in Figures 4b and 5b. The RMSF plot between ligands and COX-1/COX-2 are quite similar. Nevertheless, it is observed that complex 4b has less fluctuation than complex 5b. Figure 4c and 5c shows the number of hydrogen bonds in the interaction of GO-COX-1/2 and ARA. The GO-COX-1 and GO-COX-1 + ARA complexes had almost the same number of hydrogen bonds, as does the GO-COX-2 and GO-COX-2 + ARA.

Radius of gyration (Rg) results are shown in Figure 4d and 5d. As seen in Figure 4d, GO-COX-1 complex has less fluctuation compared to GO-COX-1 + ARA complex. The interaction of GO-COX-1 decreased the backbone Rg values till 10 ns. This was also observed in the GO-COX-1 + ARA interaction, but the Rg values increased after 10 ns.

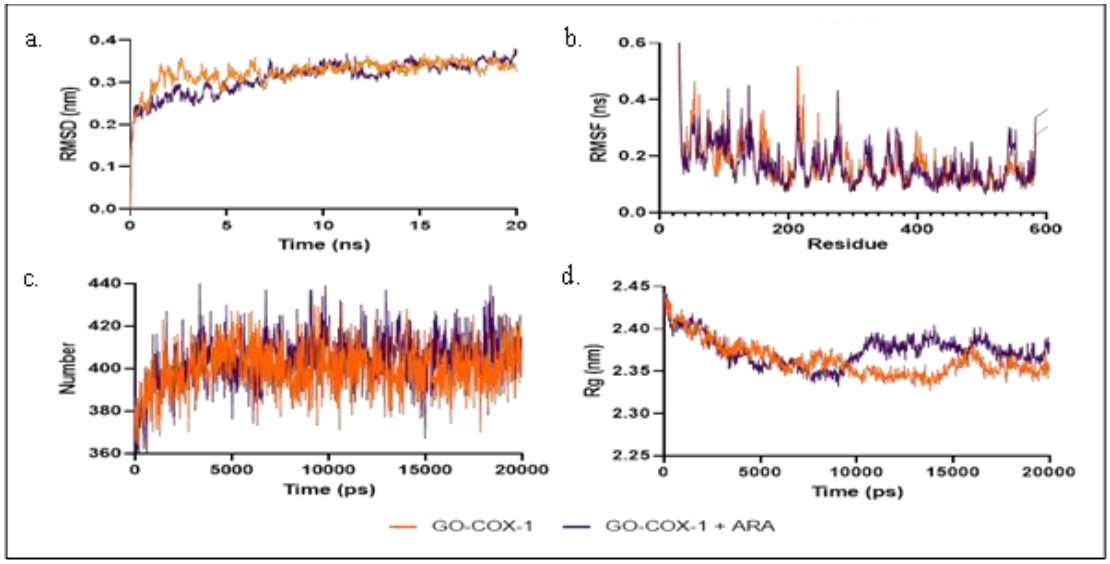

Figure 4. The molecular dynamic simulation results between GO, COX-1 and ARA. The RMSD study plot for 20 ns (a), RMSF plot (b), hydrogen bonding number study plot (c), and radius of gyration study plot (d). Orange color is the GO-COX-1 complex and the purple color is the GO-COX-1 + ARA complex.

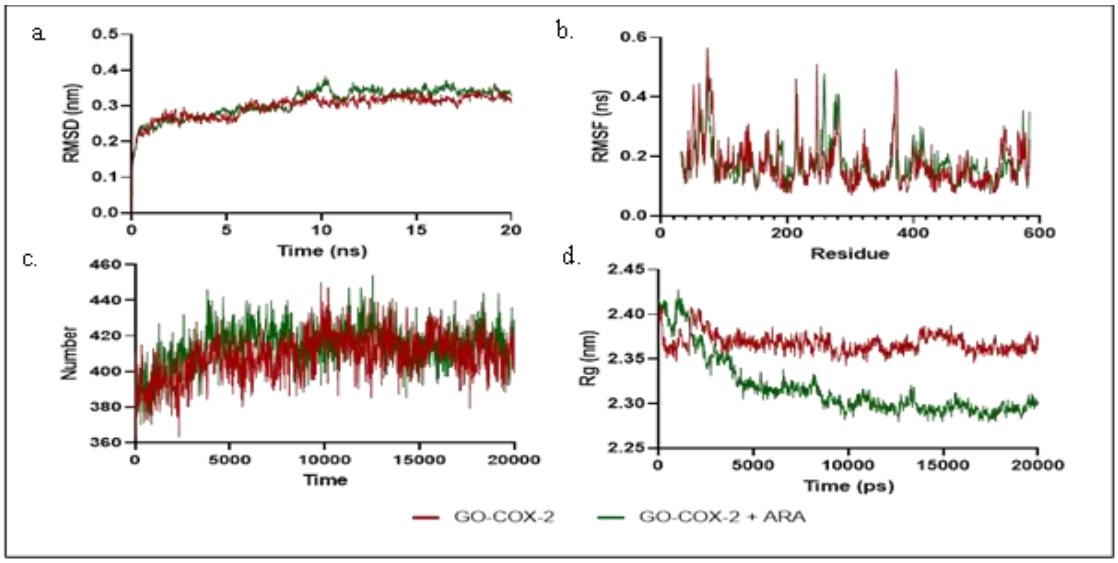

Figure 5. The molecular dynamic simulation results between GO, COX-2 and ARA. The RMSD study plot for 20 ns (a), RMSF plot (b), hydrogen bonding number study plot (c), and radius of gyration study plot (d). Red color is the GO-COX-2 complex and the purple color is the GO-COX-2 + ARA complex.

The drug likeness, biological activity, ADME, and toxicity prediction

Table 3 shows the predicted data for the biological activity of GO compounds. The GO compound has Pa > Pi values, which indicates the reaching of compound's biological active. The GO has values for anti-inflammatory (0.667 > 0.02), transcription factor NF kappa B inhibitor (0.617 > 0.033), antipruritic (0.615 > 0.014), lipid peroxidase inhibitor (0.458 > 0.022) and antioxidant (0.457 > 0.008). Based on the data obtained from analysis of the Lipinski's rules, GO obey two physicochemical parameters, the number of hydrogen-bond donor groups (nHD) ≤ 5, and the number of hydrogen-bond acceptor groups (nHA) ≤ 10 (Avdeef & Kansy, 2020). The GO is predicted to be included in toxicity class 6 which is categorized as non-toxic with an LD value of 25000mg/kg.

Table 3. Drug-likeness, ADME, biological activity, and toxicity prediction of gamma oryzanol

Drug-likeness				
Log P	**MW**	**Hydrogen Donor**	**Hydrogen Acceptor**	**n-violations**
9.23	602.90	4	1	2
ADME				
Water Solubility	**GI absorption**	**BBB**	**P-gp**	**Bioavailability Score**
1.27e-08 mg/ml (insoluble)	Low	No	Yes	0.17
Biological Activity				
Type of Activity	**Pa**		**Pi**	
Antiinflammatory	0.667		0.02	
Androgen receptor expression inhibitor	0.629		0.01	
Transcriptiom factor NF Kappa B Inhibitor	0.617		0.033	
Antipruritic	0.615		0.014	
Lipid peroxidase inhibitor	0.458		0.022	
Antioxidant	0.457		0.008	
Toxicity Prediction				
Toxicity class	**Lethal Dose**		**Category**	
6	25000mg/kg		Non-toxic	

Discussion

Molecular docking

Gamma oryzanol was bound to the COX 1 site with the same amount of interaction, compared to the ARA-COX-1 complex. The interactions of GO-COX-1 complex were dominated by hydrophobic chemical bonds. One electrostatic and many hydrophobic bonds were involved in GO-COX-1 complex. Based on molecular docking results in Figure 1b, through pi-cation electrostatic bond, the ARG120 amino acid residue of COX-1 bonded to GO. Both COX-1 and COX-2 are having identical amino acid sequences in the active sites, which are located in the hydrophobic area, near the active site cavity. Whereas, the amino acid residue ARG120 is one of the amino acids that surrounds the active site cavity of COX-1 (Ahmadi et al., 2022). An interaction between the substrate and COX-1 amino acid residue, ARG120, is essential for binding and catalysis (Smith & Malkowski, 2019). One of non-steroidal anti-inflammatory drugs (NSAID), which is ibuprofen, has a potent mechanism to inhibit the inflammation processes via COX-1 by reversibly binding to COX-1 active site cavity through ARG120 amino acid residue. Likewise, indomethacin has been reported to bind amino acids SER530, ALA527, VAL349, and LEU531 as a time-dependent COX inhibitor binding to the hydrophobic pocket (Blobaum et al., 2013). Time-dependent means that the inhibition of indomethacin on Cox activity is affected by time, with the longer the incubation time, the greater the inhibition of enzyme activity (Prusakiewicz et al., 2004).

The amino acid residues of COX-1, namely, VAL349, LEU523, ALA527, and LEU531 bind to the ARA and GO by slightly similar bond lengths. Based on our data (Fig. 1c), GO compounds lead a shifting of amino acid residue, in C=O functional group of ARA ligands interaction, from ASN 375 to HIS383, LEU 531 to LEU390, and remove the interaction between ARA with LEU527 and PHE518, which are COX-1 hydrophobic active sites that important in the biotransformation of COX-1 into prostaglandins. Nevertheless, GO-COX-1 complex has the strongest binding affinity, compared to ARA-COX-1 complex and GO-COX-1 + ARA, respectively -7.8 kcal/mol, -7.6 kcal/mol and -7.0 kcal/mol. Those data indicated that GO has a better ability to binding with COX-1 than ARA ligand. However, there is limitation in the study, that the other known inhibitor standards for COX-1 such as ibuprofen, aspirin were not docked to COX-1 to see the comparison of the effectiveness of GO among other COX-1 inhibitors.

Gamma oryzanol and COX-2 complex shows 2 hydrogen bond interactions of length respectively 2.5 Å and 3.5 Å at HIS90 and TYR91 amino acid residues. The bond length of the complex interaction is correlated to the bond strength and bond energies. The bond length of ≥ 3 Å indicates a significant interaction between ligand-receptor complexes (Joseph et al., 2015). Based on the data (Fig. 2b), the GO-COX-2 complex interacted at the same amino acid residue as the ARA-COX-2 complex through hydrogen and hydrophobic bonds with HIS90 and ARG513, in similar bonding distance. Based on the previous research, HIS90 and ARG513 were the selective pocket of the COX-2 active site (Alam et al., 2016). The ARG120 amino acid residue was not involved in the ligands and COX-2 complex interaction. The COX-2 receptor has a larger channel volume, therefore, a direct interaction between substrate and ARG120 is not a functional requirement (Smith & Malkowski, 2019).

Gamma oryzanol shifts the interaction at TYR385 residue of COX-2 and ARA (Fig. 2c). The TYR385 is transferred by an electron to an oxidized heme during enzymatic activity to initiate the cyclooxygenase reaction (Araújo et al., 2020). This reaction mechanism involves the forming of a tyrosyl radical at TYR385 amino acid residue (Raharjo et al., 2013). The interaction of a tyrosyl radical and C-13 PRO-S hydrogen of ARA formed a pentadienyl radical. In this context, GO potentially reduce the COX-2 activity as an uncompetitive inhibitor by shifting the interaction between ARA substrate with COX-2 active site.

The interaction of the ligand and COX-1/COX-2 influences the binding energy calculation (Raharjo et al., 2014). The presence of GO increases the binding energy between ARA and COX-1/COX-2. Higher binding energy can be a result of compounds inhibiting interactions (Wijayanti et al., 2022). The GO could be predicted as COX-1 inhibitor selective according to the interaction between the ligand and receptor. Tables 1 and 2 show the binding affinity calculation of GO-COX-1 is slightly higher than the GO-COX-2 complex.

Molecular dynamic simulation

The RMSD plot of GO-COX-2 and GO-COX-2 + ARA (Fig. 5a) barely shows the fluctuation between the complexes. The change in backbone of a protein indicated by the RMSD fluctuations. As showed in the figure 4a and 5a, RMSD results showed many stable plots in all complexes. The fluctuation of residual variation was analyzed by RMSF. The less fluctuation indicate that the complexes are much stable and lower energy. The complex 4b (Fig. 4) has less fluctuation than complex 5b (Fig. 5). Radius of gyration (Rg) of GO-COX-1 complex has less fluctuation compared to GO-COX-1 + ARA complex. The interaction of GO-COX-1 decreased the backbone Rg values till 10 ns. In the time between 10 and 20 ns show the more stable Rg value of all complexes (Figs. 4d and 5d). High fluctuations in Rg indicate that the conformation of the protein-ligand has a low stability and is less compact (Kalimuthu et al., 2021).

The drug likeness, biological activity, and ADME prediction

Lipinski's rule of 5 was developed to predicts the druggability of the compound. Compounds with a high probability of being drug-like molecules must follow at least two of Lipinski's rules (Benet et al., 2016). Lipinski's rule declares that an orally active drug has no more than one violation, has a molecular weight of fewer than 500, and the calculated Log P (ClogP) less than 5. Gamma oryzanol has more than 500 of molecular weight, and high lipophilicity (Log P of 9.23). Higher molecular weight and lipophilicity often contributes to low solubility, and poor oral absorption of the substance (Gao et al., 2017). Among ADME properties analysis, gamma oryzanol has a low water solubility and GI absorption. Drug solubility is one of the important indicators in ADME properties. Solubility can affect the concentration of drugs for achieving required pharmacological response. Low water soluble drugs require high doses in oral administration (Coltescu et al., 2020). In order to enhance the solubility of a compound, various physical and chemical techniques like particle size reduction, salt formation, and solid dispersion are used (Savjani et al., 2012).

According to the biological activity prediction (table 3), GO compound has activity as anti-inflammatory and transcription factor NF kappa B inhibitor. The nuclear factor kappa B (NF-kB) transcription factors has an important role to regulate inflammation responses, including COX-2. Gamma oryzanol significantly reduced lipopolysaccharide (LPS) via NF-kB transcription factor inhibition and reducing COX-2 expression (Shin et al., 2017). Likewise, GO has a strong free antioxidant activity via reactive oxygen species (ROS) scavenging by suppressing the H2O2-induced oxidative stress (Islam et al., 2009). This compound has ability to reduce the NAPDH oxidase expression by controlling the glucose-6-phosphate dehydrogenase (G6PD) (Minatel et al., 2016).

The toxicity prediction of GO revealed that this compound is non-toxic. The hepatotoxicity, carcinogenicity, mutagenicity, and cytotoxicity were included to make the prediction. Therefore, GO is suitable for use as a drug compound. Compound toxicity is critical in determining a drug candidate (Mumpuni & Mulatsari, 2018). In conclusion, gamma oryzanol of brown rice was predicted to possess a good potential to reducing inflammatory activity of COX-1 and COX-2 through binding to the COX-1 and COX-2 active site. The analysis showed that gamma oryzanol is function as a selective inhibitor of COX-1. Further experiments are required to analyzed the mechanisms of gamma oryzanol as anti-inflammation in vitro and/or in vivo.

Acknowledgement

This research was funded by the RISPRO-PRN-LPDP research grant from the Ministry of Research and Technology and the Republic of Finance, Republic of Indonesia. Author thanks to Feri Eko Hermanto for the guidance throughout this research.

References

Ahmadi, M., Bekeschus, S., Weltmann, K.-D., von Woedtke, T., & Wende, K. (2022). Non-steroidal anti-inflammatory drugs: Recent advances in the use of synthetic COX-2 inhibitors. RSC Medicinal Chemistry, 10.1039.D1MD00280E. https://doi.org/10.1039/D1MD00280E

Alam, M. J., Alam, O., Khan, S. A., Naim, M. J., Islamuddin, M., & Deora, G. S. (2016). Synthesis, anti-inflammatory, analgesic, COX1/2-inhibitory activity, and molecular docking studies of hybrid pyrazole analogues. Drug Design, Development and Therapy, 10, 3529–3543. PubMed. https://doi.org/10.2147/DDDT.S118297

Araújo, P. H. F., Ramos, R. S., da Cruz, J. N., Silva, S. G., Ferreira, E. F. B., de Lima, L. R., Macêdo, W. J. C., Espejo-Román, J. M., Campos, J. M., & Santos, C. B. R. (2020). Identification of Potential COX-2 Inhibitors for the Treatment of Inflammatory Diseases Using Molecular Modeling Approaches. Molecules (Basel, Switzerland), 25(18), 4183. PubMed. https://doi.org/10.3390/molecules25184183

Avdeef, A., & Kansy, M. (2020). Can small drugs predict the intrinsic aqueous solubility of 'beyond Rule of 5' big drugs? ADMET and DMPK, 8(3). https://doi.org/10.5599/admet.794

Benet, L. Z., Hosey, C. M., Ursu, O., & Oprea, T. I. (2016). BDDCS, the Rule of 5 and drugability. Advanced Drug Delivery Reviews, 101, 89–98. PubMed. https://doi.org/10.1016/j.addr.2016.05.007

Blobaum, A. L., Uddin, Md. J., Felts, A. S., Crews, B. C., Rouzer, C. A., & Marnett, L. J. (2013). The 2′-Trifluoromethyl Analogue of Indomethacin Is a Potent and Selective COX-2 Inhibitor. ACS Medicinal Chemistry Letters, 4(5), 486–490. https://doi.org/10.1021/ml400066a

Coltescu, A.-R., Butnariu, M., & Sarac, I. (2020). The Importance of Solubility for New Drug Molecules. Biomedical and Pharmacology Journal, 13(02), 577–583. https://doi.org/10.13005/bpj/1920

Dewi, L. (2016). In Silico Analysis of the Potential of the Active Compounds Fucoidan and Alginate Derived from Sargassum Sp. As Inhibitors of COX-1 and COX-2. Medical Archives (Sarajevo, Bosnia and Herzegovina), 70(3), 172–176. PubMed. https://doi.org/10.5455/medarh.2016.70.172-176

Francisqueti, F. V., Minatel, I. O., Ferron, A. J. T., Bazan, S. G. Z., Silva, V. D. S., Garcia, J. L., de Campos, D. H. S., Ferreira, A. L., Moreto, F., Cicogna, A. C., & Corrêa, C. R. (2017). Effect of Gamma-Oryzanol as Therapeutic Agent to Prevent Cardiorenal Metabolic Syndrome in Animals Submitted to High Sugar-Fat Diet. Nutrients, 9(12), 1299. PubMed. https://doi.org/10.3390/nu9121299

Gao, Y., Gesenberg, C., & Zheng, W. (2017). Chapter 17—Oral Formulations for Preclinical Studies: Principle, Design, and Development Considerations. In Y. Qiu, Y. Chen, G. G. Z. Zhang, L. Yu, & R. V. Mantri (Eds.), Developing Solid Oral Dosage Forms (Second Edition) (pp. 455–495). Academic Press. https://doi.org/10.1016/B978-0-12-802447-8.00017-0

Goltsov, A., Swat, M., Peskov, K., & Kosinsky, Y. (2020). Cycle Network Model of Prostaglandin H Synthase-1. Pharmaceuticals, 13(10), 265. https://doi.org/10.3390/ph13100265

Gunaydin, C., & Bilge, S. S. (2018). Effects of Nonsteroidal Anti-Inflammatory Drugs at the Molecular Level. The Eurasian Journal of Medicine, 50(2), 116–121. PubMed. https://doi.org/10.5152/eurasianjmed.2018.0010

Hongsibson, S., Sutan, K., Kerdnoi, T., & Prapamonto, T. (2016). γ-Oryzanol Content Screening in Local Brown Rice Samples from Chiang Mai, Thailand and Comparison Between Uncooked and Cooked Brown Rice. International Journal of Agricultural Research, 11(2), 84–89. https://doi.org/10.3923/ijar.2016.84.89

Islam, Md. S., Yoshida, H., Matsuki, N., Ono, K., Nagasaka, R., Ushio, H., Guo, Y., Hiramatsu, T., Hosoya, T., Murata, T., Hori, M., & Ozaki, H. (2009). Antioxidant, Free Radical–Scavenging, and NF-κB–Inhibitory Activities of Phytosteryl Ferulates: Structure–Activity Studies. Journal of Pharmacological Sciences, 111(4), 328–337. https://doi.org/10.1254/jphs.09146FP

Joseph, M., Lavinya, B., Dhinoja, S. M., Firoz, A., Das, S., Jha, M. N., Gunaseelan, D., & Sabina, E. P. (2015). In silico binding and interaction studies of inflammatory mediators in Isoniazid and Rifampicin induced toxicity against vitamin B12 and beta-carotene. Research Journal of Pharmaceutical, Biological and Chemical Sciences, 6, 1436–1440.

Kalimuthu, A. K., Panneerselvam, T., Pavadai, P., Pandian, S. R. K., Sundar, K., Murugesan, S., Ammunje, D. N., Kumar, S., Arunachalam, S., & Kunjiappan, S. (2021). Pharmacoinformatics-based investigation of bioactive compounds of Rasam (South Indian recipe) against human cancer. Scientific Reports, 11(1), 21488. https://doi.org/10.1038/s41598-021-01008-9

Krisnamurti, G. C., Research Center of Smart Molecule of Natural Genetics Resource, University of Brawijaya, Fatchiyah, F., Research Center of Smart Molecule of Natural Genetics Resource, University of Brawijaya, & Department of Biology, Faculty of Mathematics and Natural Science, University of Brawijaya. (2020). The Biological Function Prediction of The 10-gingerol Compound of Ginger in Inhibiting Cyclooxygenase-2 Activity. The Journal of Pure and Applied Chemistry Research, 9(3), 222–232. https://doi.org/10.21776/ub.jpacr.2020.009.03.547

Mastinu, A., Bonini, S. A., Rungratanawanich, W., Aria, F., Marziano, M., Maccarinelli, G., Abate, G., Premoli, M., Memo, M., & Uberti, D. (2019). Gamma-oryzanol Prevents LPS-induced Brain Inflammation and Cognitive Impairment in Adult Mice. Nutrients, 11(4), 728. PubMed. https://doi.org/10.3390/nu11040728

Minatel, I. O., Francisqueti, F. V., Corrêa, C. R., & Lima, G. P. P. (2016). Antioxidant Activity of γ-Oryzanol: A Complex Network of Interactions. International Journal of Molecular Sciences, 17(8), 1107. PubMed. https://doi.org/10.3390/ijms17081107

Mumpuni, E., & Mulatsari, E. (2018). Molecular docking and toxicity test of apigenin derivative compounds as an anti-aging agent. Journal of Applied Chemical Science, 5(1), 409–413. https://doi.org/10.22341/jacs.on.00501p409

Nafisah, W., Fatchiyah, F., Widyananda, M. H., Christina, Y. I., Rifa'ib, M., Widodo, N., & Djati, M. S. (2022). Potential of bioactive compound of Cyperus rotundus L. rhizome extract as inhibitor of PD-L1/PD-1 interaction: An in silico study. Agriculture and Natural Resources, 56(4). https://doi.org/10.34044/j.anres.2022.56.4.09

Prusakiewicz, J. J., Felts, A. S., Mackenzie, B. S., & Marnett, L. J. (2004). Molecular Basis of the Time-Dependent Inhibition of Cyclooxygenases by Indomethacin. Biochemistry, 43(49), 15439–15445.

Raharjo, S. J., Mahdi, C., Nurdiana, N., Kikuchi, T., & Fatchiyah, F. (2014). Binding Energy Calculation of Patchouli Alcohol Isomer Cyclooxygenase Complexes Suggested as COX-1/COX-2 Selective Inhibitor. Advances in Bioinformatics, 2014, 1–12. https://doi.org/10.1155/2014/850628

Raharjo, S. J., Mahdi, C., Nurdiana, N., Nellen, W., & Fatchiyah, F. (2013). Patchouli Alkohol Isomers Pogostemon Herba Predicted Virtually. Berkala Penelitian Hayati, 18(2), 98–101. https://doi.org/10.23869/bphjbr.18.2.20134

Rao, Y. P. C., Sugasini, D., & Lokesh, B. R. (2016). Dietary gamma oryzanol plays a significant role in the anti-inflammatory activity of rice bran oil by decreasing pro-inflammatory mediators secreted by peritoneal macrophages of rats. Biochemical and Biophysical Research Communications, 479(4), 747–752. https://doi.org/10.1016/j.bbrc.2016.09.140

Rouzer, C. A., & Marnett, L. J. (2003). Mechanism of Free Radical Oxygenation of Polyunsaturated Fatty Acids by Cyclooxygenases. Chemical Reviews, 103(6), 2239–2304. https://doi.org/10.1021/cr000068x

Rouzer, C. A., & Marnett, L. J. (2009). Cyclooxygenases: Structural and functional insights. Journal of Lipid Research, 50

Suppl(Suppl), S29–S34. PubMed. https://doi.org/10.1194/jlr.R800042-JLR200

Savjani, K. T., Gajjar, A. K., & Savjani, J. K. (2012). Drug solubility: Importance and enhancement techniques. ISRN Pharmaceutics, 2012, 195727–195727. PubMed. https://doi.org/10.5402/2012/195727

Shin, S. Y., Kim, H.-W., Jang, H.-H., Hwang, Y.-J., Choe, J.-S., Kim, J.-B., Lim, Y., & Lee, Y. H. (2017). γ-Oryzanol suppresses COX-2 expression by inhibiting reactive oxygen species-mediated Erk1/2 and Egr-1 signaling in LPS-stimulated RAW264.7 macrophages. Biochemical and Biophysical Research Communications, 491(2), 486–492. https://doi.org/10.1016/j.bbrc.2017.07.016

Smith, W. L., & Langenbach, R. (2001). Why there are two cyclooxygenase isozymes. The Journal of Clinical Investigation, 107(12), 1491–1495. PubMed. https://doi.org/10.1172/JCI13271

Smith, W. L., & Malkowski, M. G. (2019). Interactions of fatty acids, nonsteroidal anti-inflammatory drugs, and coxibs with the catalytic and allosteric subunits of cyclooxygenases-1 and -2. Journal of Biological Chemistry, 294(5), 1697–1705. https://doi.org/10.1074/jbc.TM118.006295

Srikaeo, K. (2014). Chapter 35—Organic Rice Bran Oils in Health. In R. R. Watson, V. R. Preedy, & S. Zibadi (Eds.), Wheat and Rice in Disease Prevention and Health (pp. 453–465). Academic Press. https://doi.org/10.1016/B978-0-12-401716-0.00035-0

Tomić, M., Micov, A., Pecikoza, U., & Stepanović-Petrović, R. (2017). Chapter 1—Clinical Uses of Nonsteroidal Anti-Inflammatory Drugs (NSAIDs) and Potential Benefits of NSAIDs Modified-Release Preparations. In B. Čalija (Ed.), Microsized and Nanosized Carriers for Nonsteroidal Anti-Inflammatory Drugs (pp. 1–29). Academic Press. https://doi.org/10.1016/B978-0-12-804017-1.00001-7

Vishvakarma, V. K., Singh, M. B., Jain, P., Kumari, K., & Singh, P. (2022). Hunting the main protease of SARS-CoV-2 by plitidepsin: Molecular docking and temperature-dependent molecular dynamics simulations. Amino Acids, 54(2), 205–213. https://doi.org/10.1007/s00726-021-03098-1

Wijayanti, E. D., Safitri, A., & Siswanto, D. (2021). Antimicrobial activity of ferulic acid in indonesian purple rice through toll-like receptor signaling. Makara Journal of Science, 25(4), 247–257. https://doi.org/10.7454/mss.v25i4.1266

Wijayanti, E. D., Safitri, A., Siswanto, D., & Fatchiyah, F. (2022). Virtual prediction of purple rice ferulic acid as anti-inflammatory of TNF-α signaling. Berkala Penelitian Hayati, 27(2), 59–66. https://doi.org/10.23869/bphjbr.27.2.20221